Genetic structure of the Japanese Robin *Larvivora akahige* endemic to East Asian islands

Journal:	*IBIS*
Manuscript ID	IBIS-2022-OA-019.R3
Wiley - Manuscript type:	Original Article (Direct Via EEO)
Category:	evolution: speciation, systematics: zoogeography, passerines, Antarctic, ecology: population genetics

Running head: Genetic structure of the Japanese Robin

Genetic structure of the Japanese Robin *Larvivora akahige* endemic to East Asian islands

SHIN-ICHI SEKI[1*]

[1] Kansai Research Center, Forestry and Forest Products Research Institute, 68 Nagaikyutaro, Momoyama, Fushimi, Kyoto, 612-0855 Japan

*Corresponding author.

Email: seki@affrc.go.jp

Geographical isolation is a key factor in allopatric speciation, but divergence with gene flow has been detected in an increasing number of studies even in island systems. To understand the divergence in island taxa, it is necessary to examine historical gene flow with mainland sister groups, which largely differ due to the various geological and ecological characteristics of each region. The Izu Islands are a chain of young and active volcanic islands in a warm-temperate climate zone that branch off from the middle of the Japanese mainland. Despite the chain's relatively limited isolation, given its proximity to the mainland, the Izu Islands feature endemic bird species and subspecies. The Japanese Robin *Larvivora akahige* is an endemic breeder on East Asian islands, and there is also a subspecies on the Izu Islands that is different in feather colouration and ecological traits. The population genetic structure of this robin was investigated using nine nuclear microsatellite markers and mitochondrial cytochrome *b* region sequences. Distinct and recent differentiation between the groups from the Izu Islands and mainland was detected from nuclear loci, although the genetic structure within the mainland group was unclear over the 1900 km habitat chain. The mitochondrial haplotypes were divided into two distant clades, one dominated throughout the robin's range and the other coexisted only on the Izu Islands as a minor type. Those clades were inferred to have diverged independent of the recent differentiation of the two nuclear clusters, although their origins and the mechanism

underlying their distribution remain unclear. The geographical characteristics of the Izu Islands may have formed a moderate but long-lasting barrier for gene flow and promoted speciation, as well as serving as a refugia for the preservation of relict lineages, particularly for migratory species which usually move along the mainland chain.

Keywords: migratory robin, island arrangement, mitonuclear discordance, relict lineage, volcanic islands

Geographical separation between populations is the initial step in allopatric speciation. Island birds have long been studied as ideal subjects of this phenomenon, because the open water between the islands forms an obvious and solid barrier for land bird species. In the classic view of allopatric speciation, geographical isolation needs to be maintained over sufficient time for the biological isolation mechanisms to develop and for the speciation process to complete (Mayr 1942, Dong *et al*. 2020). However, divergence with gene flow has been detected in an increasing number of studies even in island systems, particularly on land-bridge islands or among archipelagos, and divergence with gene flow is thought to be one of the standard processes in speciation (Grant & Grant 1996, Rheindt & Edwards 2011, Joseph 2018). Historical gene flow between allopatric populations is affected by various factors, such as the nature of the barriers (Li *et al*. 2010, Peñalba *et al*. 2017, Gyllenhaal *et al*. 2020, Manthey *et al*. 2020), the dispersal ability of the subject species (Ceresa *et al*. 2018, Cai *et al*.2020, dos Remedios *et al*. 2020), and the selection and drift that occur heterogeneously among genomic regions (Toews *et al*. 2016, Irwin e*t al*. 2018, Sendell-Price *et al*. 2021). To understand the population histories of island taxa it is necessary to untangle the available phylogeographic data and identify the major factors affecting gene flow with their mainland sisters.

The Japanese Robin *Larvivora akahige* is an endemic breeder on the East Asian islands around Japan; it inhabits Sakhalin Island, the mainland Japanese archipelago (Hokkaido, Honshu, Shikoku,

and Kyushu), and some of the smaller adjacent islands (Fig. 1; Seki *et al*. 2012). Within the robin's habitat, the Izu Islands are a short chain of volcanic islands that branches off to the south from the middle of the major habitat chain, which lies along the Japanese mainland and runs from northeast to southwest. The populations on the Izu Islands are usually treated as a separate subspecies *L. akahige tanensis*, which is distinguishable from the mainland nominate *L. akahige akahige* through certain phenotypical characteristics, particularly feather colouration (reviewed in Seki *et al*. 2012). The Izu Islands' subspecies *L. a. tanensis* is a partial migrant in lowland warm-temperate forest, whereas *L. a. akahige* is a summer visitor to deciduous and mixed coniferous forests in montane or cool-temperate regions (Nakamura & Nakamura 1995). With its unique phenotypical and ecological traits and geographically separated distribution, the subspecies in the Izu Islands has been presumed to be a well differentiated group since its initial description (Kuroda 1923, Momiyama 1923, Kuroda 1932, Ornithological Society of Japan 2012).

The results of mitochondrial DNA (mtDNA) investigation of the robin; however, have created confusion regarding this traditional classification (Seki *et al*. 2012); there are two distant mtDNA clades, with a sequence divergence of about 2.3% for the cytochrome *b* (cyt*b*) region, but the distribution of each clade does not correspond to the range of each subspecies. One dominant clade was found throughout the robin's range, whereas the other clade coexisted only on the Izu Islands as a minor type. Those two mtDNA clades are reasonably inferred to have diverged 0.7–1.6 MYA in two different refugia during the mid-Pleistocene glacial period (Seki *et al*. 2012), although the formation of the volcanic Izu Islands is estimated to date to the late-Pleistocene, approximately within 0.1 MYA for habitat islands (Kaizuka *et al*. 2000), which is younger than the formation of the clades. The minor clade now endemic to the Izu Islands may thus have a different geographical origin. It is true that the pattern of haplotype distribution indicates restricted mtDNA gene flow between subspecies, but the phenotypical traits of *L. a. tanensis* may have differentiated recently, independent of the formation of the mtDNA clades.

This study sought to reveal the population genetic structure of the Japanese Robin based on nuclear microsatellite markers and mtDNA cyt*b* sequences throughout the Japanese archipelago covering most of the robin's major habitat. Using the resulting structure and migration rate parameters, I examined how island isolation may have worked as a geological barrier restricting gene flow along the chain of young volcanic islands inhabited by the subspecies *L. a. tanensis*. To infer the history of population expansion across the Japanese Archipelago, which may be closely related to the pattern of historical gene flow, population divergence scenarios differing in the timing of expansion into the Izu Islands were compared using the approximate Bayesian computation (ABC) method. Historical changes in gene flow patterns were also discussed by superimposing the distribution of mtDNA haplotypes on a microsatellite-based structure plot.

METHODS

Sampling and DNA analysis

Blood, tissue or feathers were sampled from 292 individuals from 15 populations covering most of the breeding range of the species (Fig. 1; Table 1) from 2002–18. The sampling locations were mapped over the robin's distribution using QGIS 3.16 (QGIS.org 2021) based on the records of the national breeding bird survey (Biodiversity Center of Japan 2004). Samples collected at two locations on different islands or locations more than 100 km apart within an island were treated as belonging to different populations. Blood samples were taken from the brachial vein of the mist-netted birds, tissue samples were taken from frozen specimens of accidentally killed individuals, and both types of samples were stored in 99.5% ethanol until DNA extraction. Fallen feathers collected from mist-netted birds were provided by bird banders and stored in paper bags with silica gel pellets. Most of the samples (99.3%) were collected at the robins' breeding sites during the breeding season using mist-nets and conspecific song playback, so the samples were severely male biased (89.7% male). One

sample from a resident bird on Mikura Island collected during the non-breeding season was included as an exception, because the sample size from that island was relatively small. Total DNA was extracted using the QIAamp Micro Kit and Mini Kit (QIAGEN), following the standard protocol of each kit.

All samples were genotyped at nine polymorphic microsatellite loci using avian universal primer pairs: LTMR6 (McDonald & Potts 1994); Cuμ28 (Gibbs *et al*. 1999); Tgu02, Tgu06, and Tgu07 (Slate *et al*. 2007); TG02-088, TG03-002, and TG11-011 (Dawson *et al*. 2010); and CAM-10 (Dawson *et al*. 2013; Table S1). Universal markers were employed because they often exhibit moderate levels of polymorphism across populations from a wide geographic range, and the results are easily comparable even among related species. Candidate markers were sorted carefully beforehand because difficult peaks often appear when universal markers are used due to slight unexpected mutations around the primer range.

Polymerase chain reaction (PCR) amplification was carried out using the Type-it Microsatellite PCR Kit (QIAGEN) following the standard protocol at the final reaction mixture volume of 5 μL. Locus-specific forward primers were directly fluorescently labeled or were modified with 5' tails for universal fluorescent labeling primers (Blacket *et al*. 2012; Table S1). The thermal profile using a SimpliAmp Thermal Cycler (Applied Biosystems) consisted of initial denaturation at 95°C for 5 min, followed by 30 cycles of 95°C for 3 s; 58°C or 54°C annealing (depending on the primer pairs) for 90 s; 72°C for 30 s; and a final extension at 60°C for 40 min, then storage at 4°C. The sizes of the PCR products were read and visualized using a 3130 Genetic Analyzer, GeneScan™ 400HD ROX™ dye size standard, and scored manually in GeneMapper 5.0 (Applied Biosystems).

The partial cyt*b* region of the mtDNA for each of the individuals was amplified by PCR with the AXL149 and AXH160 primer pair (Seki 2006) and sequenced following its original protocol. Among the 292 total samples used, 53 were in common with the previous study solely based on the mtDNA sequence data (Seki *et al*. 2012), and sequences for those samples were downloaded from

GenBank. The remaining 24 samples used in Seki *et al*. (2012) were excluded from the present study because they were collected from non-breeding sites or lacked permission for further usage in microsatellite analyses; a few rare haplotypes were eliminated due to this selection, but this should not affect the overall results.

Examination of genetic diversity

The following genetic diversity indices were calculated for each of the populations, except for Toshima Island, for the microsatellite data: number of alleles per locus (*N*a), inbreeding coefficient (F_{IS}), observed and expected heterozygosities (*H*o and *H*e) using GENEPOP 4.7.5 (Rousset 2008), and allelic richness (*A*r) using FSTAT 2.9.4 (Goudet 1995). The population on Toshima Island, within the northern most group of the Izu Islands, was excluded from most of the population-based analyses because only one individual could be captured due to the low population density of the robin on this island. Departure from the Hardy–Weinberg equilibrium (HWE) for each population and locus was tested by the Markov chain method with GENEPOP. The linkage disequilibrium between each pair of loci was determined using GENEPOP. The effects of null alleles on heterozygote deficiency were evaluated with Micro-Checker 2.2.3 (van Oosterhout *et al*. 2004).

MtDNA sequences were aligned by eye, and the median joining network of haplotypes was inferred with PopArt (Leigh & Bryant, 2015). Mitochondrial genetic diversity indices, haplotype diversity (h) and nucleotide diversity (π), were calculated with Arlequin 3.5.2.2 (Excoffier & Lischer 2010). Fu's *F*s statistics, which are used to test selective neutrality and are sensitive indicators of population expansion (Fu 1997), were also evaluated with Arlequin.

Population differentiation, genetic structure, and gene flow

The conventional *F*-statistics (F_{ST}) and standardized G''_{ST} (Meirmans & Hedrick 2011) for microsatellite data between all population pairs were calculated to evaluate the genetic differentiation

among populations with GenAlEx 6.503 (Peakall & Smouse 2006). For mtDNA sequence data, F_{ST} and evolutionary distance–based $Ø_{ST}$ values and their significance were calculated with Arlequin. These values were visualized by heatmaps using the package gplots on R 4.0.3 (R Core Team 2020).

The robin's population genetic structure was examined with STRUCTURE 2.3.4 (Pritchard *et al*. 2000) based on Bayesian clustering. Ten independent runs were performed for each supposed number of genetic clusters (K = 1–5, which supposes the five clusters at maximum, corresponding to the four major islands of Japan plus the Izu Island group), for 1 000 000 Markov chain Monte Carlo (MCMC) iterations after a burn-in period of 200 000 steps, with an admixture model with sampling locations as prior information (LOCPRIOR) and the allele frequency correlated option. The most likely value of K was determined on the basis of the log-likelihood value L(K) and the second-order rate of change in the likelihood ΔK (Evanno *et al*. 2005) with the web-based program STRUCTURE Harvester 0.6.94 (Earl & von Holdt 2012). Ten independent runs for the selected K values were averaged with CLUMPP 1.1.2 (Jakobsson & Rosenberg 2007), and the resulting bar plot was visualized with DISTRUCT 1.1 (Rosenberg 2004). Under the correlated allele frequency model used in the STRUCTURE analyses, the rate of drift away from the common ancestral allele frequency (F-value) was calculated for each cluster (Falush *et al*. 2003).

Spatial structure analysis based on the autocorrelation coefficients (r) for even geographic distance classes was also performed based on the microsatellite allele frequency data using GenAlEx along the two habitat chains: one along the Japanese mainland habitats from the islands of Rishiri to Yaku, which consists of 20 geographic distance classes of 100 km each, and the other along the branch habit chain from Fuji on Honshu to Aogashima, the southernmost of the Izu Islands, which consists of five distance classes, also of 100 km each. The significance of each r value was tested using confidence intervals (CI) obtained from 999 random permutations of the geographic locations. Permutational heterogeneity tests of correlogram were performed based on Omega values (Smouse *et al*. 2008).

Contemporary and recent migration rates were examined based on the microsatellite allelic frequency data with BayesAss 3.0.4 (BA3; Wilson & Rannala 2003) and MIGRATE 3.7.2 (Beerli 2009) among the four regional population groups, the Northern, Central and Southern Japan, and the Izu Islands (see also Table 1). Four regional groups were used because using all 14 populations separately would require the estimation of a large number of parameters with limited loci and may thus fail to accurately estimate some parameters. Those four regional groups were adopted because they formed apparent geographical blocks within the robin's range, and population pairs tended to have slightly larger *F*-statistic values between groups than those within groups (see Results). BA3 was used to estimate the contemporary gene flow over the last several generations, presented as the proportion of migration derived individuals per generation (m). The program was first run at the default setting, and then the MCMC mixing parameters of allele frequencies (ΔA), inbreeding coefficients (ΔF), and migration rates (ΔM) were adjusted stepwise so that each parameter showed a moderate acceptance rate according to Wilson and Rannala (2003). After the tuning step, four independent runs were performed with the following parameter values, each with a different random number of seeds, and the resulting migration rates were averaged: $\Delta A = 0.85$, $\Delta F = 0.99$, $\Delta M = 0.85$, 10 million iterations with one million burn-in, and a sampling interval of 100.

MIGRATE, a Bayesian population genetics inference program based on structured coalescence, was used to estimate the recent migration rate (mutation-scaled migration rate: $M = m/\mu$) over a longer time period than BA3 ($4N$e generations; Beerli 2009). M values represent the importance of migration relative to mutation to increase the variability of population. The program was run with a full migration model under the default Brownian motion microsatellite datatype setting, but with some parameter modifications: the maximum theta and immigration rate values were changed to 100 and 150, respectively; the number of replicates was set to four; and each run had 10,000 recorded steps with a 20,000 burn-in, and a recorded interval of 100.

To infer the history of population expansion across the Japanese Archipelago I made use of the ABC method DIYABC 2.1.0 (Cornuet *et al*. 2014) to compare three simple divergence scenarios among the abovementioned four regional groups, all assuming that the species expanded its range northward after recent glaciation (Seki *et al*. 2012) but differing in the timing of the divergence of the Izu Islands group. The three scenarios are as follows: (1) the Izu Islands group diverged from the Central Japan group most recently; (2) the Izu Islands group diverged from the ancestral Southern Japan group in the early period of expansion; (3) all four groups radiated simultaneously (see Fig.S1a for details). The comparison of population expansion scenarios would be informative for understanding the historical gene flow patterns among regions. The scenarios were modeled using the timing of evolutionary events and effective size of each population as parameters. In all, 100 000 simulations for each scenario were performed using the default priors and values recommended in the manual. The most likely scenario was selected by comparing the logistic regression estimates of the posterior probabilities among scenarios.

RESULTS

Genetic diversity

Among the nine microsatellite loci examined, the number of alleles per locus observed ranged from three to 11, averaging 6.44 (Table S1). No significant deviation from HWE was detected within any of the populations, and none of the pairs of loci showed significant departures from linkage equilibrium after sequential Bonferroni corrections (adjusted *P*-value for 5% nominal level). Heterozygote deficiencies due to null alleles were not detected except for TG11-011 on the island of Rishiri, the northernmost of the examined populations. Brookfield estimates of null allele frequencies were less than 0.12 for all loci of all populations (Table S1), so all nine loci were used for further analyses. Microsatellite diversity indices, *N*a, *A*r, *H*o and *H*e, showed a similar tendency across populations

(Table 1); they were relatively high among the Japanese mainland populations and low among the populations in the Izu Islands and in the southernmost, Yaku Island. None of the F_{IS} values were significantly different from zero ($P < 0.05$), and ranged from −0.061 to 0.150 across the sampled sites (Table 1).

The 1007 bp of partial cyt*b* region sequences were obtained from all 292 robins, and 34 haplotypes were identified based on the 46 variable sites (Fig. 2; Table 1). Two haplotype clades, divided by at least 19 steps of sequence difference, were evident in the median joining network (Fig. 2). Clade A haplotypes were dominant in most populations, whereas clade T, which consisted of a single haplotype (T1), was observed only in the Izu Islands as a minor clade (Fig. 2 & 4a). Haplotype diversity (h) was high in the mainland Japan and Rishiri Island populations (0.64–0.89) and tended to be low in the populations on smaller islands, Yaku Island, and the Izu Islands (0.10–0.57; Table 1). Nucleotide diversity (π) also tended to be low in some island populations, but high in the Izu Island populations due to the inclusion of the outlier haplotype T1 (Table 1). Fu's F_S values were negative in the mainland and Rishiri Island populations and those values were significant for the islands of Rishiri, Tokachi and Kyushu ($P < 0.05$; Table 1).

Population differentiation, genetic structure, and gene flow

F_{ST} values based on microsatellite allelic frequency data ranged from 0.01 to 0.25 (Fig. 3a; Table S2a), and the values between populations from the Izu Islands and those from the other regions were relatively large (0.11–0.25) and significantly different from zero ($P < 0.05$). Populations on Kyushu and Yaku were also significantly different from some other mainland populations ($P < 0.05$), but all F_{ST} values were less than 0.06 between those pairs. Standardized G''_{ST} values showed a similar tendency (Fig. 3b; Table S2a); they were large and significant between the populations on the Izu Islands and the rest of the populations ($P < 0.05$), although the total range expanded from −0.03 to 0.54. MtDNA haplotype frequency based F_{ST} was significant ($P < 0.05$) for those pairs of populations

between Yaku Island and all other regions and ranged from 0.42 to 0.86 (Fig. 3c; Table S2b). Twenty of the 32 pairs between the Izu Island and mainland populations were significantly different from zero ($P < 0.05$), with F_{ST} values larger than 0.1. $Ø_{ST}$ values using the Kimura 2-parameter model defined evolutionary distances among haplotypes again exhibited significant differentiation between Yaku Island and all other regions (0.45–0.82, $P < 0.05$; Fig. 3d; Table S2b). The pairs between mainland populations and other islands populations, the Izu Islands, or Rishiri Island, often had significant $Ø_{ST}$ values ($P < 0.05$), but the values differed widely among population pairs, ranging from 0.05 to 0.36.

In the STRUCTURE clustering analysis, the most likely number of clusters was two, which expressed the greatest values for both L(K) and ΔK (Table S3). The individual Q-matrix showed that all individuals captured or collected in the Izu Islands were inferred to have a higher ancestry probability for cluster II, being 92.0% on average and 53.4% at the least (Fig. 4b). Overall ancestry probability for cluster II tended to be high in the southern part of the Izu Islands, which is farthest from the Japanese mainland. The majority of the Japanese mainland individuals exhibited a higher ancestry probability for cluster I, with an average of 83%, although some individuals had values less than 50%. The average F-value from ten independent runs was higher in cluster II ($F_{II} = 0.507$) than in cluster I ($F_{I} = 0.034$).

The correlograms of both the mainland and branching habitat chains showed a significant spatial structure ($P = 0.002$ and $P = 0.001$, respectively). Among the 10 populations along the mainland habitat chain, significantly positive spatial autocorrelation coefficient (r) values were obtained in the smallest two distant classes—that is, within 200 km (Fig. 5a). For distance classes larger than two, significantly negative values appeared for three distance classes, 500, 800 and 1900 km, although the rest of the classes had slightly positive or negative non-significant r values. Among the five populations of the branching chain, the first 100 km distance class had a significantly positive r value, and the last three classes, larger than 200 km, had significantly negative values, which decreased as the distance increased (Fig. 5b).

Contemporary migration rates inferred by BA3 were low overall between the Izu Islands and the other groups; the proportion of migratory individuals in the Izu Islands derived from either mainland group was inferred to be less than 1% (posterior mean proportion 0.4–0.5%), and the 95% CIs in each case included 0% in the range (Table 2a). In the mainland groups, 0.8–1.5% of individuals were inferred to be migrants derived from the Izu Islands, and again all 95% CIs included 0% in the range. Migration rates were mostly less than 5% also among the mainland groups (the upper limits of the 95% CIs slightly increased to 14.1% but their lower limits were 0%), although migrants from central Japan to northern Japan or to southern Japan accounted for 28.6% and 25.6% of individuals, respectively.

Recent gene flow estimated by MIGRATE with microsatellite data showed an asymmetric pattern between southern Japan and the other three regions (Table 2b). The *M* values to southern Japan from the other three regions ranged from 10.4 to 17.7 representing the top three *M* values, whereas gene flows in the opposite direction were inferred to be lower, with *M* values of 1.9 to 5.8. The migration parameter among the Izu Islands, northern Japan and central Japan exhibited moderate *M* values, ranging from 4.7 to 8.8.

Among the three divergence scenarios examined in DIYABC analysis, the third scenario of simultaneous radiation of all four groups was selected as most likely, having the highest posterior probability of 0.983 (median value; 95% CI = 0.978 –0.988; Fig. S1b). Under scenario three, the median time of the divergence among the four groups was estimated to be 243 generations ago (95% range = 119–471) under the default model used in DIYABC (Fig. S2). The median of the posterior estimate of the present effective population size of the Izu Islands group was 429 (95% range of posterior distribution = 264–2340), much smaller than for the other three groups (5880 for northern Japan [95% range = 1850–9320]; 6880 for central Japan [95% range = 2600–9590]; 3690 for Southern Japan [95% range = 1350–6610]).

DISCUSSION

Genetic structure using autosomal markers

Distinct differentiation in microsatellite allelic frequency was detected between the Japanese Robins from the Izu Islands and from the Japanese mainland, which is concordant with the subspecies boundary based on phenotypic traits. Both the conventional and standardised *F*-statistics were large when population from the Izu Islands were compared with the mainland. In the STRUCTURE analysis, most of the individuals from the Japanese mainland were inferred to have a higher ancestry probability for cluster I whereas the majority of the Izu Islands' individuals exhibited a higher ancestry probability for cluster II. Contemporary gene flow between these pairs of regions was estimated to be rare. The divergence scenario that best explained the data in the ABC analyses; however, was the recent simultaneous radiation of all regions, not the older isolation of the Izu Islands or northward stepwise expansion. On caveat is that the support for the preferred scenario of simultaneous radiation across the species range, may in part be a result of insufficient resolution of the present microsatellite datasets to discriminate the quick stepwise expansion, especially if this was recent and happened over a short period of time. The low genetic diversity, relatively large inbreeding coefficients, and higher *F*-value for the dominant cluster of the Izu Islands are also consistent with the inference of recent differentiation of the Izu Islands group from the ancestral mainland group, independent of the older divergence of the two mtDNA clades reported in a previous study (Seki *et al*. 2012). The timing of the radiation suggested from DIYABC analysis was 119–471 generations ago, which could be converted to roughly within 1300 years using a generation time of 2.7 years (average value from the data of Muscicapidae in Bird *et al*. 2020), but could be much older because DIYABC tends to considerably underestimate the timing of demographic events (Cornuet *et al*. 2010, Tsuda *et a*l. 2015, Cabrera & Palsbøll 2017).

After such geologically recent simultaneous radiation, only the Izu Islands group exhibited distinct genetic differentiation from the other groups. The smaller effective population size of the Izu

Islands group, which was inferred to be nearly one order of magnitude smaller than those of all other mainland groups in the DIYABC analysis, may have affected the distinct genetic characteristics of this group though increased genetic drift. Another important factor would be isolation from the mainland, although isolation-by-distance alone would not fully explain the observed patterns. Even within the mainland subspecies range, the robins' preference for the montane or the cool-temperate forests limits its present habitat to island-like patches (Seki *et al*. 2012), and the habitat isolation distances within the mainland subspecies are rather larger than those between the two subspecies. Nevertheless, the genetic structure among mainland populations was unclear over the 1900 km habitat chain, whereas the isolation-by-distance effect was evident and highly significant among the Izu Islands populations. Island isolation along the branching habitat chain of the Izu Islands may have worked differently than simple isolation-by-distance effects along the major chain. The difference in migratory habits among subspecies may have caused this difference in the isolation effect. The mainland subspecies is a summer visitor who migrates along the mainland habitat chain that runs from the northeast to southwest. However, the subspecies on the Izu Islands is a partial migrant (resident individuals are common, but the proportion is unidentified), and even migratory individuals may require a drastic change in their migration route. Migrants on the Izu Islands are assumed to move northward from their breeding grounds before joining the mainland migration route toward the southwest (see Fig. 1). Distinct genetic differentiation between populations with different migratory behaviours has been widely reported among passerine birds (e.g. Alvarado *et al*. 2014, Delmore & Irwin 2014, Contina *et al*. 2019), and the geographic location of the Izu Islands, which requires a initial reversal of migratory direction followed by a right-angle turn to the south, may promote the robin's genetic differentiation beyond a simple isolation-by-distance effect.

Migratory movement may have another effect on the pattern of gene flow. Contemporary gene flow estimated with BA3 was low overall among the groups, except for those from the central Japan group to the neighboring northern and southern Japan groups. The results using the program

MIGRATE; however, were different. The *M* values, indicating the importance of migration relative to mutation in the long-term increase in genetic variability, suggested higher levels of gene flow into the southern Japan group from the other three groups but not vice versa. This asymmetrical pattern may be related to the effect of migration on dispersal. Migration is a regular seasonal movement and is ecologically different behaviour from dispersal, but migratory species often disperse further than resident species (Paradis *et al*. 1998) and gene flow along the main migration axis can occasionally be greater (Chabot 2011). Long-distance or infrequent successful dispersal to a suitable habitat along the migration route south of the natal site would lead to higher southward gene flow over a longer time scale. Regular short-distance dispersal, infrequent long-distance movement related to migration, and the historical northward expansion could explain the present obscure genetic structure among the mainland groups.

Mitonuclear discordance on the Izu Islands

The geographic distributions of the two distant mtDNA clades of the Japanese Robin, which were inferred to have diverged from glacial refugia in the mid-Pleistocene (Seki *et al*. 2012), were reinvestigated for a larger number of individuals from a wider region covering most of the species' range. Once more the major clade (clade A) was found throughout the robin's range, whereas the minor clade (clade T) was restricted to the Izu Islands. Moreover, clade T consisted of a small number of haplotypes, with only one haplotype in the present study and another reported in a previous study (Seki *et al*. 2012), whereas clade A consisted of up to 33 haplotypes. Another noticeable characteristic of the clade distribution is that clade T was found on all six sampled islands within the Izu Islands chain, whereas it has never been found in mainland populations. Within the Izu Islands, clade T was observed even on very small islands, such as Toshima (4.1 km^2 in area and 48 km from a neighbouring island habitat; Center for Research and Promotion of Japanese Islands 2019) and Aogashima (6.0 km^2 and 64 km, respectively), despite the larger effect of genetic drift on such small

islands. As a result, mitonuclear discordance was observed only on the Izu Islands, and on all sampled islands.

The origin of clade T mtDNA and the mechanism underlying its distribution remain unclear. One possible factor affecting such a clade distribution is natural selection acting on mitochondrial respiration efficiency, which is expected to work strongly in high-altitude montane habitats (Graham *et al*. 2018) or in populations with long-distance migratory habits (Toews *et al*. 2014). Compared with the island subspecies, which inhabits lowland warm-temperate forests as a partial migrant, the mainland subspecies of the robin, which breeds in montane or boreal cool-temperate forests as a summer visitor, is likely exposed to different selective pressures on mitochondrial respiration efficiency. Persistence of the minor mtDNA clade even on small islands within the Izu Islands region is another confusing phenomenon, but may possibly be affected by the timing of the population contact or balancing selection working in those islands. Further integrative research on the differences in mtDNA respiration efficiency of the two clades, their genetic background based on the larger genome datasets, and the differences in ecological requirements among robins in different environments will be needed to reveal the species history and robustly explain the present distribution pattern of the two mtDNA clades.

Avian endemism in the Izu Islands

There are other endemic or near endemic bird species and subspecies in the Izu Islands other than this subspecies of robin and they exhibit various levels of genetic differentiation from their sister taxa on the mainland. The Varied Tit *Sittiparus varius* for example, is a resident forest dweller in East Asia, and two of its subspecies, *S. v. namiyei* and *S. v. owstoni*, are endemic to the northern and southern Izu Islands, respectively (Ornithological Society of Japan 2012). These island subspecies have distinctive plumage and morphometric characteristics and are inferred to have recently differentiated from mainland subspecies as a result of two successive colonization events based on the microsatellite data

(Fujita *et al*. 2014). From mtDNA sequence data, the two subspecies are both placed within a well-supported monophyletic clade together with the mainland subspecies (McKay *et al*. 2014), which supports the recent differentiation of these groups.

The Izu Thrush *Turdus celaenops* is another resident species mostly endemic to the Izu Islands, although it also has a small remote population in the Tokara Islands in southern Japan. Recent mtDNA analysis has revealed that the thrush forms a shallow monophyletic clade, but it also forms a super-species clade with the migratory Brown-headed Thrush *T. chrysolaus* which is widely distributed in East Asia; there was only one diagnostic substitution between the two species among 648 bp of Cytochrome c Oxidase I region sequences (Saitoh *et al*. 2015). It appears uncontroversial that the Izu Thrush was differentiated from its mainland sister relatively soon after the formation of the islands.

The migratory Iijima's Leaf Warbler *Phylloscopus ijimae* also breeds only in the Izu Islands and the Tokara Islands. Based on four mitochondrial and nuclear region sequences, the warbler in the Izu Islands has formed a monophyletic clade that was placed as the closest sister of the Eastern Crowned Warbler *P. coronatus* on the mainland (Alström *et al*. 2018). The estimated divergence time between the two species was; however, more than 3 MYA—that is, far older than the age of the Izu Islands, which date to around 0.1 MYA (Kaizuka *et al*. 2000). The warblers are inferred to have differentiated somewhere on the mainland in the Pliocene, and Iijima's Leaf Warbler might have become extinct in its original habitat and remained only in limited islands' regions.

Solely from the mtDNA analysis of the robin (Seki *et al.* 2012), clade T appeared to be a confusing foreign genetic piece that only indicates a restriction in gene flow between the Izu Islands and mainland. Together with the nuclear microsatellite information, the distribution of the mtDNA clades suggests the presence of a moderate but long-lasting barrier for gene flow between the two regions. Further examples of endemic birds in the studied regions indicate the restriction of gene flow in various groups of birds. The geological, geographical, and environmental characteristics of the Izu

Islands, a young volcanic island chain with a warm climate that branches off to the south of mainland Japan, may have enhanced the effects of physical isolation and differences in selective pressure with the mainland. Future research examining the genetic, physiological, and ecological background of the present pattern of mitonuclear discordance in the Japanese Robin may also facilitate the understanding of the formation of other endemic groups of birds in the region.

I would like to thank Manabu Kajita, Gen Morimoto, Kazuto Kawakami, Takeshi Ogura, and Isao Nishiumi for generously providing some of the samples; and Keiko Hamaguchi, Naoki Ohnishi, and Yasuyuki Ishibashi for technical assistance in the laboratory. I am also grateful to Takema Saitoh, Yuji Okahisa, Yasuko Iwami, Katsumi Tamada, Hajime Takano, Hiroyoshi Higuchi, Keisuke Ueda, Hiroshi Uchida, Michio Matsuda, Hiroshi Kawase, Kazuyuki Tsukahara, Masahiko Sakanashi, Yutaka Nakamura, Fumio Mizoguchi, Kazunobu Kogi, Shigeho Sato, Yoshinori Suzuki, Teruaki Hino, and Hitoshi Tojo for offering local information about the robin. In addition, I would like to thank the regional forest offices of the Forest Agency of Japan for their support and the permission to conduct fieldwork in the national forest. Finally, I am grateful to the editors Rauri Bowie and Martin Stervander, as well as the two anonymous reviewers for their insightful comments that improved the quality of this work.

CONFLICT OF INTEREST

None.

ETHICS AND PERMITTING

The subject species was captured and sampled with the permission of the Ministry of the Environment of Japan.

FUNDING

This study was partially supported by JSPS KAKENHI Grant Number JP21370039, JP26450208, and JP21K05696.

AUTHOR CONTRIBUTION

Shin-Ichi Seki: Conceptualization (Lead); Data curation (Lead); Funding acquisition (Lead); Investigation (Lead); Project administration (Lead); Resources (Lead); Visualization (Lead); Writing – original draft (Lead); Writing – review & editing (Lead).

DATA AVAILABILITY STATEMENT

All sequence data have been deposited in the DDBJ nucleotide data bank (Accession No. LC666763–796; Table S4). The analyses reported in this article can be reproduced using those sequences and the genotyping data provided in the Table S5.

REFERENCES

Alström, P., Rheindt, F.E., Zhang, R., Zhao, M., Wang, J., Zhu, X., Gwee, C. Y., Hao, Y., Ohlson, J., Jia, C., Prawiradilaga, D.M., Ericson, P.G.P., Lei, F. & Olsson, U. 2018. Complete species-level phylogeny of the leaf warbler (Aves: Phylloscopidae) radiation. *Mol. Phylogenet. Evol.* 126: 141–152.

Alvarado, A.H., Fuller, T.L. & Smith, T.B. 2014. Integrative tracking methods elucidate the evolutionary dynamics of a migratory divide. *Ecol. Evol*. 4: 3456–3469.

Beerli, P. 2009. How to use MIGRATE or why are Markov chain Monte Carlo programs difficult to use. *Popul. Genet. Anim. Conserv.* 17: 42–79.

Biodiversity Center of Japan 2004. *Report of the Distributional Survey of Japanese Animals (Birds)*. Fujiyoshida: Biodiversity Center of Japan (in Japanese).

Bird, J.P., Martin, R., Akçakaya, H.R., Gilroy, J., Burfield, I.J., Garnett, S.T., Symes, A., Taylor, J., Şekercioğlu, C.H. & Butchart, S.H. 2020. Generation lengths of the world's birds and their implications for extinction risk. *Conservation Biology* 34: 1252–1261.

Blacket, M., Robin, C., Good, R., Lee, S. & Miller, A. 2012. Universal primers for fluorescent labelling of PCR fragments—An efficient and cost-effective approach to genotyping by fluorescence. *Mol. Ecol. Res.* 12: 456–463.

Cabrera, A.A. & Palsbøll, P.J. 2017. Inferring past demographic changes from contemporary genetic data: A simulation-based evaluation of the ABC methods implemented in DIYABC. *Mol. Ecol. Res.* 17: e94–e110.

Cai, T., Shao, S., Kennedy, J.D., Alström, P., Moyle, R.G., Qu, Y., Lei, F. & Fjeldså, J. 2020. The role of evolutionary time, diversification rates and dispersal in determining the global diversity of a large radiation of passerine birds. *J. Biogeogr.* 47: 1612–1625.

Center for Research and Promotion of Japanese Islands 2019. *SHIMADS*. Tokyo: Center for Research and Promotion of Japanese Islands (in Japanese).

Ceresa, F., Belda, E.J., Kvist, L., Kajanus, M. & Monrós, J.S. 2018. Genetic differentiation between insular and continental populations of migratory and resident warblers, the Great Reed Warbler *Acrocephalus arundinaceus* and Cetti's Warbler *Cettia cetti*. *J. Ornithol.* 159: 703–712.

Chabot, A.A. 2011. The Impact of Migration on the Evolution and Conservation of an Endemic North American Passerine: Loggerhead Shrike (*Lanius ludovicianus*). *Ph.D. Thesis*. Kingston: Queen's University.

Contina, A., Alcantara, J.L., Bridge, E.S., Ross, J.D., Oakley, W.F., Kelly, J.F. & Ruegg, K.C. 2019. Genetic structure of the Painted Bunting and its implications for conservation of migratory populations. *Ibis* 161: 372–386.

Cornuet, J.-M., Pudlo, P., Veyssier, J., Dehne-Garcia, A., Gautier, M., Leblois, R., Marin, J.-M. & Estoup, A. 2014. DIYABC v2.0: a software to make approximate Bayesian computation inferences about population history using single nucleotide polymorphism, DNA sequence and microsatellite data. *Bioinformatics* 30: 1187–1189.

Cornuet, J.-M., Ravigné, V. & Estoup, A. 2010. Inference on population history and model checking using DNA sequence and microsatellite data with the software DIYABC (v1.0). *BMC Bioinformatics* 11: 401.

Dawson, D.A., Ball, A.D., Spurgin, L.G., Martín-Gálvez, D., Stewart, I.R., Horsburgh, G.J., Potter, J., Molina-Morales, M., Bicknell, A.W., Preston, S.A., Ekblom, R., Slate, J. & Burke, T. 2013. High-utility conserved avian microsatellite markers enable parentage and population studies across a wide range of species. *BMC Genom*. 14: 1–22.

Dawson, D.A., Horsburgh, G.J., Küpper, C., Stewart, I.R., Ball, A.D., Durrant, K.L., Hansson, B., Bacon, I., Bird, S., Klein, A., Krupa, A.P., Lee, J.-W., Martín-Gálvez, D., Simeoni, M., Smith, G., Spurgin, L. & Burke, T. 2010. New methods to identify conserved microsatellite loci and develop primer sets of high cross-species utility—as demonstrated for birds. *Mol. Ecol. Res.* 10: 475–494.

Delmore, K.E. & Irwin, D.E. 2014. Hybrid songbirds employ intermediate routes in a migratory divide. *Ecol. Lett*. 17: 1211–1218.

Dong, F., Li, S.-H., Chiu, C.-C., Dong, L., Yao, C.-T. & Yang, X.-J. 2020. Strict allopatric speciation of sky island *Pyrrhula erythaca* species complex. *Mol. Phylogenet. Evol*. 153: 106941.

Earl, D.A. & vonHoldt, B.M. 2012. STRUCTURE HARVESTER: A website and program for visualizing STRUCTURE output and implementing the Evanno method. *Conserv. Genet. Res*. 4: 359–361.

Evanno, G., Regnaut, S. & Goudet, J. 2005. Detecting the number of clusters of individuals using the software STRUCTURE: A simulation study. *Mol. Ecol*. 14: 2611–2620.

Excoffier, L. & Lischer, H.E. 2010. Arlequin suite ver 3.5: A new series of programs to perform population genetics analyses under Linux and Windows. *Mol. Ecol. Res*. 10: 564–567.

Falush, D., Stephens, M. & Pritchard, J.K. 2003. Inference of population structure using multilocus genotype data: linked loci and correlated allele frequencies. *Genetics* 164: 1567–1587.

Fu, Y.-X. 1997. Statistical tests of neutrality of mutations against population growth, hitchhiking and background selection. *Genetics* 147: 915–925.

Fujita, K., Nishiumi, I., Yamaguchi, N., Fujita, G. & Higuchi, H. 2014. Spatial structure and colonization process of Varied Tit populations in the Izu Islands. *Ornithol. Sci*. 13: 91–107.

Gibbs, H.L., Tabak, L.M. & Hobson, K. 1999. Characterization of microsatellite DNA loci for a neotropical migrant songbird, the Swainson's thrush (*Catharus ustulatus*). *Mol. Ecol*. 8: 1551–1551.

Goudet, J. 1995. FSTAT (version 1.2): A computer program to calculate F-statistics. *J. Hered*. 86: 485–486.

Graham, A.M., Lavretsky, P., Muñoz-Fuentes, V., Green, A.J., Wilson, R.E. & McCracken, K.G. 2018. Migration-selection balance drives genetic differentiation in genes associated with high-altitude function in the speckled teal (*Anas flavirostris*) in the Andes. *Genome Biol. Evol*. 10: 14–32.

Grant, P.R. & Grant, B.R. 1996. Speciation and hybridization in island birds. *Philos. Trans. R. Soci. B: Biol. Sci*. 351: 765–772.

Gyllenhaal, E.F., Mapel, X.M., Naikatini, A., Moyle, R.G. & Andersen, M.J. 2020. A test of island biogeographic theory applied to estimates of gene flow in a Fijian bird is largely consistent with neutral expectations. *Mol. Ecol*. 29: 4059–4073.

Irwin, D.E., Milá, B., Toews, D.P., Brelsford, A., Kenyon, H.L., Porter, A.N., Grossen, C., Delmore, K.E., Alcaide, M. & Irwin, J.H. 2018. A comparison of genomic islands of differentiation across three young avian species pairs. *Mol. Ecol*. 27: 4839–4855.

Jakobsson, M. & Rosenberg, N.A. 2007. CLUMPP: A cluster matching and permutation program for dealing with label switching and multimodality in analysis of population structure. *Bioinformatics* 23: 1801–1806.

Joseph L. 2018. Phylogeography and the role of hybridization in speciation. In Tietze, D.T. (ed) *Bird Species: How They Arise, Modify and Vanish*: 165–194. Heidelberg: Springer Verlag.

Kaizuka S., Koike, K., Endo, K., Yamazaki, H. & Suzuki, T. 2000. *Regional Geomorphology of the Japanese Islands 4: Geomorphology of Kanto and Izu-Ogasawara*. Tokyo: University of Tokyo Press (in Japanese).

Kuroda, N. 1923. *Erithacus akahige tanensis*, subsp. nov. *Bull. Brit. Ornithol. Club* 153: 106.

Kuroda, N. 1932. A revision of the types of birds described by Japanese authors during the years 1923 to 1931. *Novit. Zool*. 37: 384–405.

Leigh, J.W. & Bryant D. 2015. PopART: Full-feature software for haplotype network construction. *Meth. Ecol. Evol*. 6: 1110–1116.

Li, J.-W., Yeung, C.K., Tsai, P.-W., Lin, R.-C., Yeh, C.-F., Yao, C.-T., Han, L., Hung, L.M., Ding, P. & Wang, Q. 2010. Rejecting strictly allopatric speciation on a continental island: Prolonged postdivergence gene flow between Taiwan (*Leucodioptron taewanus*, Passeriformes Timaliidae) and Chinese (*L. canorum canorum*) hwameis. *Mol. Ecol*. 19: 494–507.

Manthey, J.D., Oliveros, C.H., Andersen, M.J., Filardi, C.E. & Moyle, R.G. 2020. Gene flow and rapid differentiation characterize a rapid insular radiation in the southwest Pacific (Aves: *Zosterops*). *Evolution* 74: 1788–1803.

Mayr, E. 1942. *Systematics and the Origin of Species*. New York: Columbia University Press.

McDonald, D.B. & Potts, W.K. 1994. Cooperative display and relatedness among males in a lek-mating bird. *Science* 266: 1030–1032.

McKay, B.D., Mays Jr, H.L., Yao, C.-T., Wan, D., Higuchi, H. & Nishiumi, I. 2014. Incorporating color into integrative taxonomy: Analysis of the varied tit (*Sittiparus varius*) complex in East Asia. *Syst. Biol*. 63: 505–517.

Meirmans, P.G. & Hedrick P.W. 2011. Assessing population structure: FST and related measures. *Mol. Ecol. Res*. 11: 5–18.

Momiyama, T.T. 1923. *Erithacus akahige sgectatoris*, subsp. nov. *Doubutsugaku Zasshi* 35: 403–404 (in Japanese).

Nakamura, T. & Nakamura, M. 1995. *Birds' Life in Japan with Color Pictures: Birds of Mountain, Woodland and Field*. Osaka: Hoikusha (in Japanese).

van Oosterhout, C., Hutchinson, W.F., Wills, D.P. & Shipley, P. 2004. MICRO-CHECKER: software for identifying and correcting genotyping errors in microsatellite data. *Mol. Ecol. Notes* 4: 535–538.

Ornithological Society of Japan 2012. *Check-list of Japanese Birds, 7th Revised Edition*. Sanda: Ornithological Society of Japan.

Paradis, E., Baillie, S.R., Sutherland, W.J. & Gregory, R.D. 1998. Patterns of natal and breeding dispersal in birds. *J. Anim. Ecol*. 67: 518–536.

Peakall, R. & Smouse, P.E. 2006. GENALEX 6: genetic analysis in Excel. Population genetic software for teaching and research. *Mol. Ecol. Notes* 6: 288–295.

Peñalba, J.V., Mason, I.J., Schodde, R., Moritz, C. & Joseph, L. 2017. Characterizing divergence through three adjacent Australian avian transition zones. *J Biogeogr*. 44: 2247–2258.

Pritchard, J.K., Stephens, M. & Donnelly, P. 2000. Inference of population structure using multilocus genotype data. *Genetics* 155: 945–959.

QGIS.org 2021. *QGIS Geographic Information System*. QGIS Association. http://www.qgis.org

R Core Team 2020. *R: A language and environment for statistical computing (Version 4.0.3)*. Vienna: R Foundation for Statistical Computing. http://www.R-project.org

dos Remedios, N., Küpper, C., Székely, T., Zefania, S., Burns, F., Bolton, M., & Lee, P.L. 2020. Genetic structure among *Charadrius* plovers on the African mainland and islands of Madagascar and St Helena. *Ibis* 162: 104–118.

Rheindt, F.E. & Edwards, S.V. 2011. Genetic introgression: An integral but neglected component of speciation in birds. *Auk* 128: 620–632.

Rosenberg, N.A. 2004. DISTRUCT: a program for the graphical display of population structure. *Mol. Ecol. Notes* 4: 137–138.

Rousset, F. 2008. genepop'007: A complete re-implementation of the genepop software for Windows and Linux. *Mol. Ecol. Res*. 8: 103–106.

Saitoh, T., N. Sugita, N., Someya, S., Iwami, Y., Kobayashi, S., Kamigaichi, H., Higuchi, A., Asai, S., Yamamoto, Y. & Nishiumi, I. 2015. DNA barcoding reveals 24 distinct lineages as cryptic bird species candidates in and around the Japanese Archipelago. *Mol. Ecol. Res*. 15: 177–186.

Seki, S.-I. 2006. The origin of the East Asian Erithacus robin, *Erithacus komadori*, inferred from cytochrome *b* sequence data. *Mol. Phylogenet. Evol*. 39: 899–905.

Seki, S.-I., Nishiumi, I. & Saitoh, T. 2012. Distribution of two distinctive mitochondrial DNA lineages of the Japanese Robin *Luscinia akahige* across its breeding range around the Japanese islands. *Zool. Sci*. 29: 681–689.

Sendell-Price, A.T., Ruegg, K.C., Robertson, B.C. & Clegg, S.M. 2021. An island-hopping bird reveals how founder events shape genome-wide divergence. *Mol. Ecol*. 30: 2495–2510.

Slate, J., Hale, M.C. & Birkhead, T. R. 2007. Simple sequence repeats in zebra finch (*Taeniopygia guttata*) expressed sequence tags: a new resource for evolutionary genetic studies of passerines. *BMC Genom*. 8: 1–12.

Smouse, P. E., Peakall, R. & Gonzales, E. 2008. A heterogeneity test for fine-scale genetic structure. *Mol. Ecol*. 17: 3389–3400.

Toews, D.P., Brelsford, A., Grossen, C., Milá, B. & Irwin, D.E. 2016. Genomic variation across the Yellow-rumped Warbler species complex. *Auk* 133: 698–717.

Toews, D.P., Mandic, M., Richards, J.G. & Irwin, D.E. 2014. Migration, mitochondria, and the yellow-rumped warbler. *Evolution* 68: 241–255.

Tsuda, Y., Nakao, K., Ide, Y. & Tsumura, Y. 2015. The population demography of *Betula maximowicziana*, a cool-temperate tree species in Japan, in relation to the last glacial period: its admixture-like genetic structure is the result of simple population splitting not admixing. *Mol. Ecol*. 24: 1403–1418.

Wilson, G.A. & Rannala, B. 2003. Bayesian inference of recent migration rates using multilocus genotypes. *Genetics* 163: 1177–1191.

Table 1. Genetic diversity estimates of 14 Japanese Robin populations: number of alleles per locus (*N*a), allelic richness (*A*r), observed and expected heterozygosities (*H*o and *H*e), and inbreeding coefficient (F_{IS}) for microsatellite data, and number of haplotypes (*N*h), haplotype diversity (*h*), nucleotide diversity (π), and Fu's *F*s statistics of selective neutrality for mtDNA data. Asterisks indicate significant values at the $P < 0.05$ significance level.

Region	Sampling sites	*n*	Microsatellites				MtDNA			
			*N*a	*A*r	*H*o/*H*e	F_{IS}	*N*h	*h* ± SD	π ± SD (%)	Fu's *F*s
Northern	1. Rishiri Is.	26	4.44	3.77	0.48/0.49	0.038	9	0.67 ± 0.10	0.11 ± 0.08	-5.20*
Japan	2. Tokachi	30	4.56	3.83	0.48/0.49	-0.007	9	0.76 ± 0.06	0.14 ± 0.10	-3.58*
	3. Kushiro	21	4.11	3.51	0.45/0.42	0.089	8	0.87 ± 0.04	0.19 ± 0.12	-2.26
Central	4. Ohu	13	3.89	3.85	0.52/0.54	0.004	7	0.87 ± 0.07	0.20 ± 0.13	-2.34
Japan	5. Nikko	17	3.89	3.56	0.45/0.47	-0.011	5	0.64 ± 0.12	0.16 ± 0.11	-0.22
	6. Fuji	34	5.00	4.05	0.49/0.50	0.027	11	0.86 ± 0.04	0.22 ± 0.14	-3.22
	7. Kii	14	4.44	4.28	0.52/0.51	0.060	8	0.91 ± 0.05	0.22 ± 0.15	-2.94
Southern	8. Shikoku Is.	15	4.44	4.24	0.54/0.52	0.069	6	0.76 ± 0.08	0.17 ± 0.12	-1.24
Japan	9. Kyushu Is.	12	4.00	4.00	0.48/0.45	0.096	8	0.89 ± 0.08	0.21 ± 0.14	-3.82*
	10. Yaku Is.	23	3.22	2.95	0.39/0.38	0.057	2	0.17 ± 0.10	0.03 ± 0.04	0.77
Izu Islands	11. Miyake Is.	28	2.67	2.35	0.22/0.19	0.150	2	0.45 ± 0.07	0.92 ± 0.48	18.42
	12. Mikura Is.	12	2.56	2.56	0.18/0.17	0.120	2	0.48 ± 0.11	0.98 ± 0.54	12.55
	13. Hachijo Is.	26	2.22	2.07	0.17/0.19	-0.061	3	0.57 ± 0.08	0.77 ± 0.41	12.56
	14. Aogashima Is.	20	1.78	1.72	0.13/0.12	-0.048	2	0.10 ± 0.09	0.20 ± 0.13	5.34

Table 2. Rates of gene flow between the four population groups based on microsatellite data. (a) Contemporary gene flow estimated using BayesAss, expressed as the posterior mean proportion of migrants (*m*). (b) Recent gene flow estimated using MIGRATE over a longer time period presented as the posterior median of the mutation-scaled migration rate ($M = m/\mu$). Numbers in brackets are 95% CIs.

Recipient group	Source group Northern Japan	Central Japan	Southern Japan	Izu Islands
(a)				
Northern Japan	0.693 (0.629-0.757)	0.286 (0.206-0.366)	0.014 (0.000-0.049)	0.009 (0.000-0.024)
Central Japan	0.052 (0.000-0.141)	0.929 (0.835-1.000)	0.012 (0.000-0.033)	0.008 (0.000-0.022)
Southern Japan	0.042 (0.000-0.127)	0.256 (0.156-0.355)	0.688 (0.657-0.718)	0.015 (0.000-0.041)
Izu Islands	0.004 (0.000-0.013)	0.005 (0.000-0.013)	0.004 (0.000-0.011)	0.987 (0.973-1.000)
(b)				
Northern Japan	–	7.3 (3.3-10.8)	4.8 (1.6-7.6)	5.3 (1.8-8.4)
Central Japan	5.7 (1.9-9)	–	5.8 (1.8-9.1)	8.8 (4.9-12.2)
Southern Japan	14.1 (5.7-19.6)	17.7 (5.3-22.5)	–	10.4 (6.1-14.6)
Izu Islands	4.7 (1.6-7.5)	8.0 (4.2-11.2)	1.9 (0.0-4.0)	–

Figure Captions

Figure 1. Distribution of the Japanese Robin and sampling locations. Tree marks indicate approximately 400 km^2 square cells where the robin was recorded during the breeding season in the period 1997–2002 by the distributional survey of Japanese birds (Biodiversity Center of Japan 2004). Black circles indicate sampling locations from regional populations.

Figure 2. Median joining haplotype network of the Japanese Robin based on the mtDNA cyt*b* sequences. Two major clades of haplotypes divided by 19 steps of sequence difference are framed with gray lines. Each circle represents a unique haplotype as colour-coded pie chart by populations and the size corresponds to its frequency. Each line between haplotypes indicates a single mutational step and inferred haplotypes are shown with black dots.

Figure 3. Heatmap of the pairwise values of genetic differentiation among populations. (a) F_{ST} and (b) G''_{ST} based on microsatellite allelic frequency data, (c) F_{ST} based on mtDNA haplotype frequencies and (d) Φ_{ST} based on K2-p distances among mtDNA haplotypes. The darker colour indicates larger value, according to the strength in the top right box of each heatmap. Population numbers are in common with Table 1 and detailed values are shown in Table S2.

Figure 4. MtDNA clade discrimination and ancestry probabilities in two nuclear clusters for each individual Japanese Robin. (a) MtDNA cyt*b* clade membership of each individual is colour-coded, clade A in red (dark) and clade T in yellow-green (light). Haplotypes included in each clade are in common with Fig. 2. (b) Ancestry probabilities in each of the two genetic clusters inferred by STRUCTURE analysis are shown in the bar plot. Bars are sampled individuals and grouped by populations. The length of red (dark) and yellow-green (light) segments indicate inferred proportion assignment to cluster I and II.

Figure 5. Spatial genetic structure of the Japanese Robin in the Izu Islands (a) and the Japanese mainland (b) based on the autocorrelation coefficient calculated for even geographic distance classes of 100 km. Each error bar is bootstrapped 95% CI for a specific distance class. Dashed lines indicate upper and lower confidence limits, representing the 95% CI under the assumption of no spatial structure for the entire distance class.

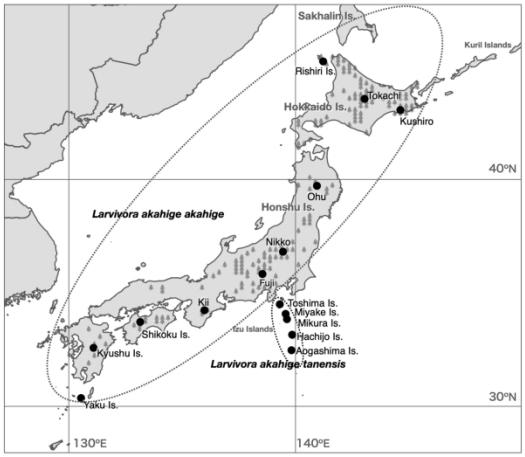

Figure 1. Distribution of the Japanese Robin and sampling locations. Tree marks indicate approximately 400 km^2 square cells where the robin was recorded during the breeding season in the period 1997–2002 by the distributional survey of Japanese birds (Biodiversity Center of Japan 2004). Black circles indicate sampling locations from regional populations.

244x346mm (300 x 300 DPI)

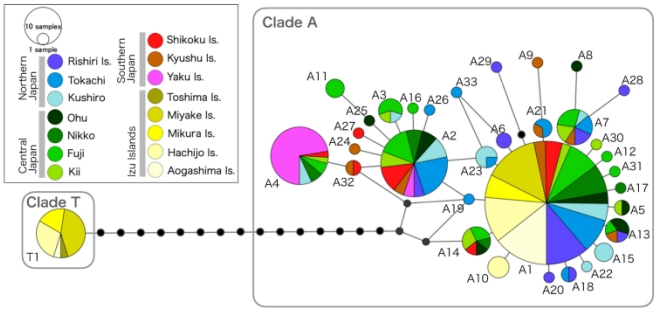

Figure 2. Median joining haplotype network of the Japanese Robin based on the mtDNA cyt*b* sequences. Two major clades of haplotypes divided by 19 steps of sequence difference are framed with gray lines. Each circle represents a unique haplotype as colour-coded pie chart by populations and the size corresponds to its frequency. Each line between haplotypes indicates a single mutational step and inferred haplotypes are shown with black dots.

244x346mm (300 x 300 DPI)

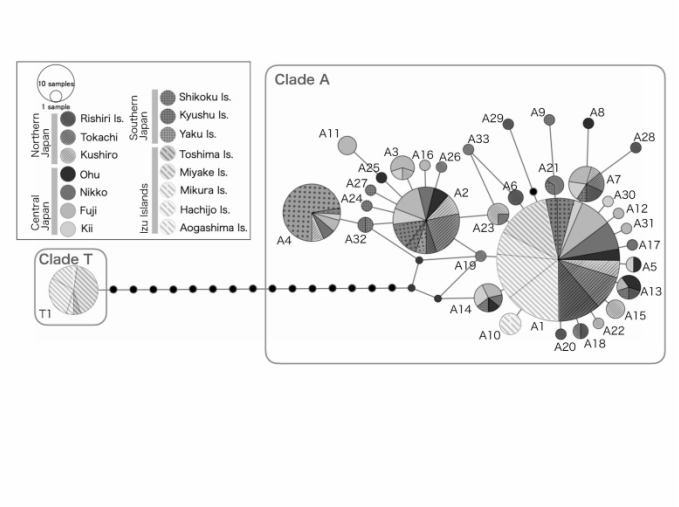

Figure 2. black and white

245x346mm (300 x 300 DPI)

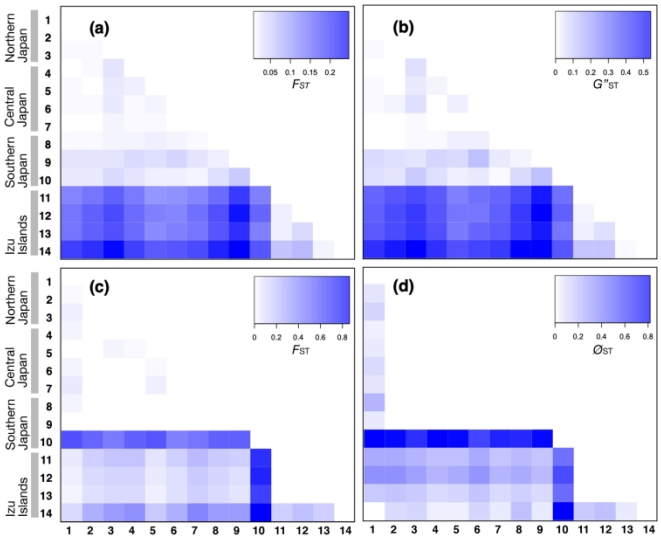

Figure 3. Heatmap of the pairwise values of genetic differentiation among populations. (a) F_{ST} and (b) G''_{ST} based on microsatellite allelic frequency data, (c) F_{ST} based on mtDNA haplotype frequencies and (d) $Ø_{ST}$ based on K2-p distances among mtDNA haplotypes. The darker colour indicates larger value, according to the strength in the top right box of each heatmap. Population numbers are in common with Table 1 and detailed values are shown in Table S2

244x346mm (300 x 300 DPI)

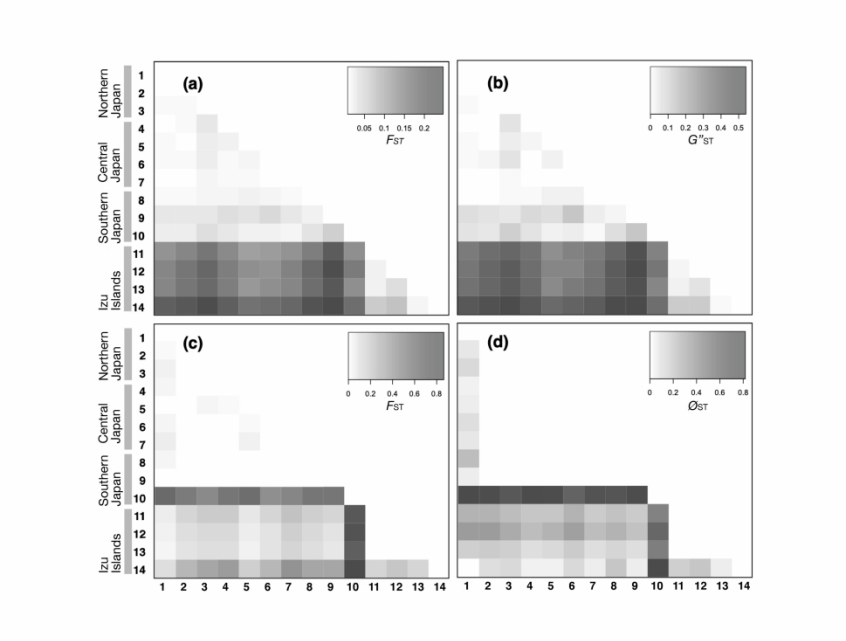

Figure 3. black and white

243x345mm (300 x 300 DPI)

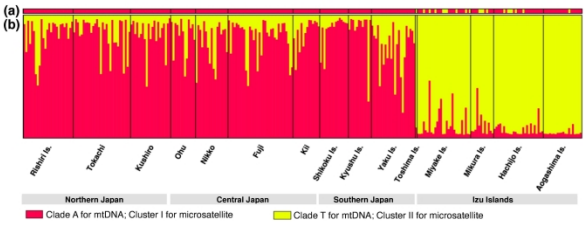

Figure 4. MtDNA clade discrimination and ancestry probabilities in two nuclear clusters for each individual Japanese Robin. (a) MtDNA cyt*b* clade membership of each individual is colour-coded, clade A in red (dark) and clade T in yellow-green (light). Haplotypes included in each clade are in common with Fig. 2. (b) Ancestry probabilities in each of the two genetic clusters inferred by STRUCTURE analysis are shown in the bar plot. Bars are sampled individuals and grouped by populations. The length of red (dark) and yellow-green (light) segments indicate inferred proportion assignment to cluster I and II.

244x347mm (300 x 300 DPI)

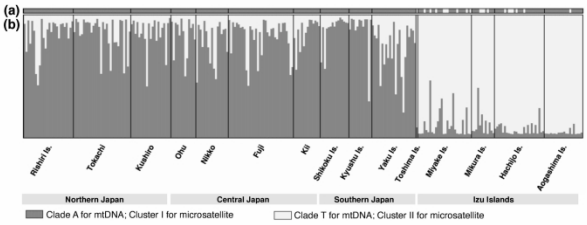

Figure 4. black and white

244x346mm (300 x 300 DPI)

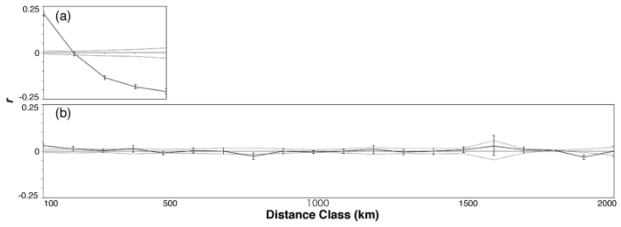

Figure 5. Spatial genetic structure of the Japanese Robin in the Izu Islands (a) and the Japanese mainland (b) based on the autocorrelation coefficient calculated for even geographic distance classes of 100 km. Each error bar is bootstrapped 95% CI for a specific distance class. Dashed lines indicate upper and lower confidence limits, representing the 95% CI under the assumption of no spatial structure for the entire distance class.

244x346mm (300 x 300 DPI)